Diagnostic value of chest computed tomography scan based on artificial intelligence and deep learning in children with lobar pneumonia and analysis of image features before and after treatment: A retrospective cohort study

L. Chen#, S. Dong#, Y. Chen*, L. Tian, C. He, S. Tao

Department of Paediatrics, Wuhan Fourth Hospital, Wuhan City, Hubei Province, China. 430033

► *Original article*

#these authors have contributed equally to this work and share first authorship.

ABSTRACT

Background: A retrospective cohort study was conducted to analyze the diagnostic value and image features of chest computed tomography (CT) scan in children with lobar pneumonia (LP) before and after treatment. ***Materials and Methods:*** 172 children with lobar pneumonia treated from January 2016 to December 2021 were selected. The patients who underwent plain X-ray scan were divided into control group (n = 72) and the patients who underwent chest CT scan as study group (n = 100). The diagnostic value and image characteristics before and after treatment were compared between the two groups. ***Results:*** After treatment, the lesion area of the patient was absorbed in varying degrees, and the CT plain scan indicated that the solid shadow density decreased until it was completely absorbed. The sensitivity, specificity, accuracy, positive predictive value and negative predictive value of chest X-ray were 66.67%, 58.33%, 63.89%, 76.19% and 46.67% respectively; and chest CT scan were 82.98%, 67.92%, 75.00%, 69.64% and 81.82%. The sensitivity, specificity, accuracy, and negative predictive value of chest CT plain scan were higher, and the positive predictive value was lower compared to those of chest X-ray plain film. The results of ROC curve study indicated that the AUC of chest CT plain scan was 0.755 (95%CI=0.657 -0.852), and the AUC of chest X-ray film was 0.625 (95%CI= 0.489-0.744). ***Conclusion:*** Chest CT has high sensitivity and specificity in the diagnosis of LP in children, which can clearly demonstrate the imaging features of LP before and after treatment.

INTRODUCTION

Lobar pneumonia is an acute pulmonary inflammatory disease caused by bacteria infection. Diplococcus pneumonia has been identified as the primary pathogen responsible for this condition [1]. Epidemiological studies has revealed that lobar pneumonia is predominantly prevalent during the winter and autumn seasons, with a higher incidence rate observed among younger patients, particularly those aged between 0-3 years, who often present with concurrent viral infections, leading to an overall increase in the number of cases [2]. With the continuous change of the living environment and the main body of the disease, the proportion of lobar pneumonia caused by Streptococcus pneumoniae infection gradually decreases, while the number of lobar pneumonia caused by other bacteria, mycoplasma and other pathogens gradually increases, which is also one of the main factors leading to atypical and changeable clinical symptoms of patients with lobar pneumonia [3-4]. Imaging examination is one of the main means to diagnose and detect lobar pneumonia in clinic. Imaging examination plays an important role in the initial diagnosis and follow-up evaluation of lobar pneumonia in children [5]. At present, the main imaging examinations include chest X-ray, computed tomography (CT) scan and so on [6-7].

Many scholars believe that X-ray plain film is the first choice for patients with lobar pneumonia because of its short time and simple operation, but some scholars hold the opposite opinion [8]. It is considered that X-ray plain film examination is a simple two-dimensional image, which lacks a comprehensive display of atypical imaging findings of lobar pneumonia and is prone to misdiagnosis and missed diagnosis [9]. Chest X-ray examination has a high rate of non-specificity and missed diagnosis, and the detection rate of airway foreign bodies is only 73.9% [10]. In recent years, with the continuous progress and development of imaging technology, chest CT plain scan has been widely used in clinic. CT examination time is short, multi-directional imaging and high image quality, obvious advantages in intuitive, multi-window display of different lung segments of the imaging findings.

CT can effectively detect and diagnose a variety of pulmonary diseases, but the physical development of children is not mature. Some patients' CT plain scan

images and X-ray plain film imaging signs are not obvious, affecting patients to receive treatment in time [11-13]. CT plain scan images of lobar pneumonia in children is not typical, observation of single lung texture increase, edge blur, consolidation and other image features cannot be qualitatively diagnosed, easy to be misdiagnosed as lobar atelectasis. Lobar atelectasis is a lobar disease, but the volume of lobar pneumonia is smaller than that of lobar pneumonia, and the adjacent organs are shifted to the lesion area. CT scan of lobar pneumonia in consolidation stage shows that dense consolidation is mostly distributed along the lobes and lung segments, and "air bronchus sign" is often seen in it [14]. Most patients actually start from the periphery of the lung lobe and close to the pleura, and then gradually spread out to the center of the lung field. According to this characteristic, we can make differential diagnosis between them [15-16]. A retrospective cohort study was conducted to analyze the diagnostic value and image features of chest CT scan in children with LP, with the aim of further exploring their efficacy before and after treatment.

MATERIALS AND METHODS

Study population

A total of 172 children with LP treated in our hospital from January 2016 to December 2021 was selected. The patients who underwent plain X-ray scan were divided into control group (n = 72) and the patients who underwent chest CT scan as study group (n = 100). In the control group, the age was 3-14 years old, with an average of (6.35 ±1.73) years, including 31 males and 41 females, while in the study group, the age was 3-14 years old, with an average of (6.69 ±1.56) years, including 56 males and 44 females. There exited no statistical significance in the general data. This study was endorsed by the Medical Ethics Association of Wuhan Fourth Hospital (2018-KY-08), and all patients signed informed consent.

Table 1. The baseline data of the patients.

Items	Control group	Study group
Sample size (n)	72	100
Males(n)	31	56
Females(n)	41	44
Age(years)	6.35 ±1.73	1.56

Inclusion criteria

Age was 3-14 years old;

2 patients who met the diagnostic criteria of MP infection, the diagnostic criteria were as follows: fever, severe cough, shortness of breath and other clinical manifestations; lung auscultation thickened breath sound, audible wet rale, local respiratory sound decreased or disappeared on the affected side, and percussion of the focus indicated voiced or solid sound; chest imaging examination: a lung segment or

even a lobe of lung or even one side of the whole lung indicated large dense shadow and so on.

3 segmental or lobar pulmonary parenchyma infiltration on chest X-ray or chest CT.

4 the pulmonary function examination was completed during hospitalization, and the quality control was good.

Exclusion criteria

1. In accordance with the diagnostic criteria of bronchial asthma and allergic rhinitis;

2. Complicated with cardiovascular diseases, thoracic malformations, bronchiolitis obliterans, neuromuscular system diseases and other diseases affecting pulmonary function;

3. Patients have contraindications for fiberoptic bronchoscope operation and being uncooperative or unable to tolerate the operator;

4. Incomplete case data.

Research methodology

Patients in both groups were given acetylcysteine for inhalation (manufacturer: Hainan Lingkang Pharmaceutical Co., Ltd.; Registration No. H20140449) Aerosol inhalation therapy, 3mL/ time, 2 times /d; Budesonide suspension (manufacturer: Sichuan Puruite Pharmaceutical Co., Ltd.; The registration number is H20140475, and the specification is 1mg: 2 mL), and the dose is 0.5mg/ (ml times) for children under 2 years old and 1mg/ (2ml times) for children over 2 years old. All patients were treated continuously for 1 week.

Control group

Radiographic analysis was performed using Siemens MultixSelectDR machine (Siemens, Germany). Sets appropriate exposure conditions according to the patient's body shape and specific conditions. The center line is aimed at the fourth thoracic vertebra, and iodine contrast agent is injected horizontally through the midpoint of the connecting line between the lower corners of the scapula on both sides, and then inhaled deeply and exposed with breath held. If necessary, take a side view and was aimed horizontally through the midpoint of the inferior corner of the scapula on both sides. Inhale deeply and expose under breath holding. Add lateral position if necessary. Adjust the target distance to 100-160 cm. Set parameters to 125 kV, 125 mA, and 0.04-0.06 s. Examination results were analyzed by two senior diagnostic imaging physicians with 10 years of work experience using double-blind method.

Study group

The CT equipment adopts Toshiba Aquilion 64-row spiral CT machine in Japan. The examinee is in supine position, and those who are young or have anxiety are accompanied by the patient's family for

CT plain scan and told the patient to breathe smoothly. CT scan range: from the bottom of the lung to the tip of the lung. Scanning parameters: tube voltage 120KV, tube current 40mA, scanning pitch 0.875, layer thickness 4mm, layer spacing 4mm, matrix: 512 × 512, mediastinal window and lung window are scanned. Window width and window position can be adjusted according to the patient's personal condition. In this study, the data were randomly divided into training set (named chest Xray_train), verification set (named chest_Xray val) and test set (named chest_Xray_test), in which 236 patients' images were used as the training set of the model, including 452 pneumonia and 242 normal images; 295 samples were used as the validation set, including 170 samples of pneumonia and 125 samples of normal, and the validation set was used to select the best training model.

Finally, the remaining 399 samples were used as an independent internal test set, including 282 pneumonia samples and 117 normal samples, to test the performance of the model. The three data sets are independent of each other. Firstly, the basic model is trained on the training data set, the best model is selected by the verification set, the superparameter is determined, the overall performance of the model is evaluated by the internal test set, and the external data is further used for testing. Based on the test results of the external test set, the model is evaluated and fine-tuned to make it more suitable for the actual data set. The SurgiPro diagnosis system is developed and designed for thoracic surgeons, which focuses on the clinical judgment of pulmonary diseases and assists thoracic surgeons in making treatment decisions; and the DICOM images of chest CT (layer thickness ≤ 1.25 mm) are imported into the two systems to record the accurate probability of diagnosis of LP in children automatically reported by the SurgiPro diagnosis system.

SurgiPro endows CT with the ability to predict pathological classification by analyzing the CT data and pathological data characteristics of patients during the same period, assisting doctors in grasping the optimal surgical opportunity before surgery, and enhancing their confidence in operation. SurgiPro can realize Iterative reconstruction of all pulmonary nodules, intuitively reflect the spatial relationship between nodules, tissues and nodules, and make doctors' diagnosis more intuitive and three-dimensional.

The "ScrynPro™-Intelligent Auxiliary Screening System for Pulmonary Nodules V3.3" and "SurgiPro™-Intelligent Auxiliary Decision System for Pneumonia V3.0.1" used in this study are from relevant technology companies, and they obtained the national CFDA medical device registration certificate (Class II) on August 8, 2018, with the registration number: Jiangxi Machinery ZhuZhuZhun 20182210153; Artificial intelligence uses the data of nearly 150,000 cases of lung CT in top-level lung specialist hospitals and well-known top-level hospitals to train artificial intelligence models, and the detection sensitivity of pulmonary nodules is ≥ 97.1%; He won the first place in the 2017 "Tianchi Medical AI Competition-Intelligent Diagnosis Competition for Pulmonary Nodules".

Observation index

Sensitivity, specificity, accuracy, positive predictive value and negative predictive value were used. The formulas for calculating sensitivity, specificity, accuracy, positive predictive value and negative predictive value are as follows:

Sensitivity= number of true positives/ (number of true positives+ number of false negatives) × 100%

Specificity= number of true negatives/ (number of true negatives+ number of false positives) × 100%

Accuracy= right number/total number × 100%

Positive predictive value (PPV) = True Positives/ (True Positives+ False Positives) × 100%

Negative predictive (NPV) = True Negatives/ (True Negatives+ False Negatives) × 100%

Statistical analysis

The data were analyzed by SPSS26.0 and MedCalc19.0.7 statistical software, the sensitivity and specificity were used to evaluate, and the positive likelihood ratio and negative likelihood ratio were calculated. The positive likelihood ratio ≥ 10 and the negative likelihood ratio ≤0.10 were considered to be of high diagnostic value. The counting data were expressed in frequency and percentage, and the paired chi-square test was used to compare the inter-group rates. The diagnostic accuracy of each group was evaluated by using the receiver working characteristic (ROC) curve and the area under ROC curve (AUC). The results indicated that AUC at 0.5-0.7 indicated lower accuracy, >0.7-0.9 had certain accuracy, and >0.9 had higher accuracy. The difference was considered to be statistically significant (P<0.05).

RESULTS

Imaging features of LP before and after treatment with chest X-ray plain film and CT plain scan

Among the 172 patients with LP, 14 patients with congestive stage indicated no obvious abnormal changes in chest X-ray, only localized lung texture increased and lung field transparency decreased slightly. The chest X-ray plain film of the patients in consolidation stage indicated a large area of uniform and consistent increased density, the appearance and scope of which were the same as those of the involved lobes and segments, and the "air bronchus sign" appeared. After treatment, the density of pulmonary window was significantly lower than that

202

Int. J. Radiat. Res., Vol. 22 No. 1, January 2024

before treatment, showing irregular distribution of dotted and patchy shadows, and only a small amount of striped shadow appeared in patients with better absorption.

In 172 patients with LP, the lesion of LP in congestive phase indicated ground glass density shadow, and the edge of the lesion area was blurred. During consolidation phase, CT indicated that dense consolidation shadow was distributed along the lung lobe and lung segment, in which "air bronchus sign" was often seen. Most of the patients manifested from the periphery of the lung lobe and close to the pleura, and then gradually spread to the center of the lung field. After treatment, the lesion area of the patient was absorbed in varying degrees, and the CT plain scan indicated that the solid shadow density decreased until it was completely absorbed.

Table 2. The varied imaging findings within the 172 cases with LP

	Without abnormal changes (n=14)	Lesion of LP in congestive phase
Pre-therapy		
Congestive stage	Only a localized increase in lung texture and a slight decrease in transparency of the pulmonary region	Ground glass density shadow, and the blurred edge of the lesion
Consolidation stage	Chest X-ray "air bronchus sign"	CT "air bronchus sign"
Post-therapy	The density of the lung window is significantly reduced, with irregularly distributed dotted and patchy shadows.	The patient's lesion is absorbed, and CT plain scan shows a decrease in solid shadow density until it is completely absorbed.

Note: LP, lobar pneumonia; CT, Computed Tomography

Diagnostic effect of chest CT plain scan and chest X-ray plain film

The sensitivity, specificity, accuracy, positive predictive value and negative predictive value of chest X-ray plain film were 66.67%, 58.33%, 63.89%, 76.19% and 46.67% respectively. The sensitivity, specificity, accuracy, positive predictive value and negative predictive value of chest CT were 82.98%, 67.92%, 75.00%, 69.64% and 81.82% respectively. The sensitivity, specificity, accuracy and negative predictive value of chest CT plain scan were higher, and the positive predictive value was lower compared to those of chest X-ray plain film. All the results are shown in table 3.

Table 3. Diagnostic effect of chest CT plain scan and chest X-ray plain film [n/%]

Index	Sensitivity	Specificity	Accuracy	Positive predictive value	Negative predictive value
X -ray	66.67 (32/48)	58.33 (14/24)	63.89 (46/72)	76.19 (32/42)	46.67 (14/30)
CT	82.98 (39/47)	67.92 (36/53)	75.00 (75/100)	69.64 (39/56)	81.82 (36/44)
χ^2	3.346	0.667	2.478	0.515	10.058
P	0.067	0.413	0.115	0.472	0.001

Note: CT, Computed Tomography.

Analysis of imaging features of clinical cases

The imaging features are shown in figure 1-2. The male patient, 3 years old, complained of fever for 1 days and cough for 2 weeks. The re-examination was significantly improved after one week of anti-infective treatment. Before treatment, CT plain scan indicated large patchy high-density shadow in Right middle lobe of the right lung of the right lung (figure 1A), After treatment, CT lung window indicated that most of the large patchy high-density shadow in Right middle lobe of the right lung disappeared, with only a few striped high-density shadows (figure 1B), suggesting that the LP of the right lung was significantly improved after treatment.
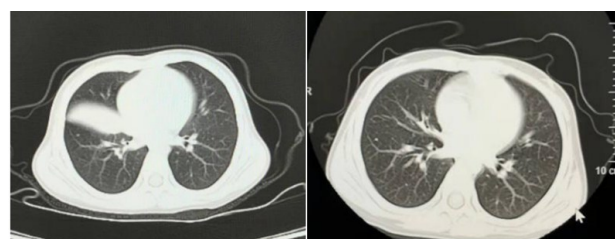

Figure 1. Imaging features of clinical cases A. CT image demonstrates that large patchy high-density shadow in right middle lobe; B. CT image demonstrates that few striped high-density shadows.

Analysis of ROC curve of chest CT plain scan and chest X-ray plain film

The results of ROC curve study indicated that the AUC of chest CT plain scan was 0.755 (95%CI = 0.657-0.852), and the AUC of chest X-ray film was 0.625 (95%CI = 0.486-0.764). The difference was statistically significant (P<0.05) figure 2.
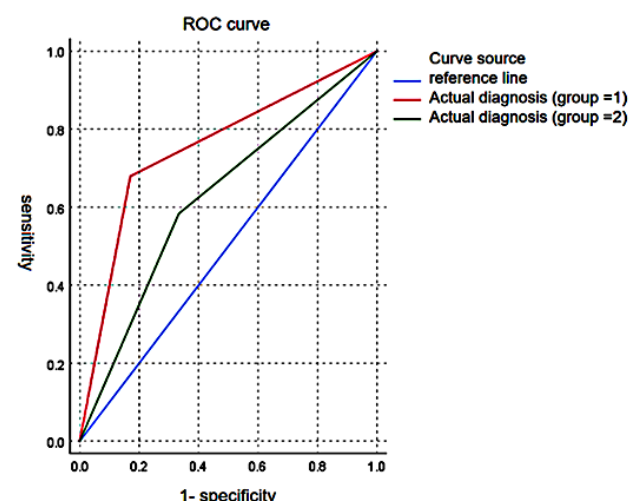

Figure 2. ROC curve analysis of chest CT plain scan and chest X-ray plain film. ROC, Receiver Operating Characteristic Curve; CT, Computed Tomography.

Typical cases before and after machine diagnosis

The results of machine learning diagnosis showed that the bilateral thorax was symmetrical and the trachea and mediastinum were centered. Both lungs are clear in texture and normal in shape, mottled blurred shadows are seen in the left upper lung, and

some of them are consolidated, but no obvious abnormal density shadows are found in the other lungs. Trachea and bronchus are unobstructed, and no obvious abnormality is found in heart and great vessels. No obvious swollen lymph nodes were found in mediastinum and bilateral armpits. No obvious hydrops was found in both chest cavities. Decreased liver density (figure 3 A-B).
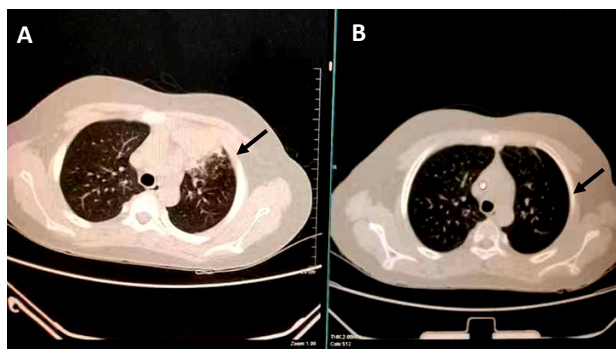

Figure 3. Typical cases before and after machine diagnosis. **A** Typical cases before machine diagnosis; **B**. Typical cases after machine diagnosis.

DISCUSSION

Lobar pneumonia (LP) is a condition characterized by pulmonary inflammation resulting from various etiologies, including pathogens, physical and chemical factors, immune injury, allergy, and drugs. Its primary clinical manifestations include fever, cough, shortness of breath, dyspnea, and fixed wet rales in the lungs. LP is considered one of the four major pediatric diseases [1]. Up to now, pneumonia represents 28-34% of the deaths of children under 5 years old worldwide. Nearly 155 million children (<5 years old) suffer from pneumonia every year, of which 11-20 million (7-13%) require hospitalization, which places a heavy burden on medical institutions [1]. Lobar pneumonia (LP) is a prevalent form of community-acquired pneumonia (CAP) in childhood. LP is an acute inflammatory condition that manifests as diffuse cellulose exudation in the alveoli, primarily alveolitis, affecting multiple lung segments [12]. It has been reported that in recent years, the incidence of LP in children is increasing year by year, and has its particularity, often lack of clinical characteristics of adult typical LP and so on [13]. With the application of broad-spectrum antibiotics, the rate of drug resistance increases, and the etiology also changes. Of note, LP is no longer limited to Streptococcus pneumoniae (SP), but becomes a single or mixed infection of bacteria, viruses, atypical pathogens and fungi, which makes the clinical symptoms of LP more complex [17].

Common pathogens of LP in children include bacteria, viruses, atypical pathogens, as well as fungi

and protozoa [18-19]. Currently, there is a lack of precise reporting on the clinical features of children with LP resulting from diverse pathogens. Notably, the clinical characteristics of LP in children vary across different age groups, particularly between infants and school-aged children [21]. LP is not only a common pathogen of LP in school-age and preschool children, but also in 1-3-year-old infants [22]. In addition, LP may be one of the independent or mixed pathogens of severe LP. The main manifestations of LP are as follows: at the beginning of the disease, general discomfort, fatigue, headache, high fever, body temperature often up to 39 ℃, and can be accompanied by sore throat and muscle soreness. Cough is a prominent manifestation of the disease, which is characterized by irritating dry cough at first and then intractable severe cough [23]. The manifestation of lung signs in children is not deemed significant, as some may present with wheezing and lung rales, which may be transient in nature, thereby rendering the symptoms and signs incongruent with the defining features of the ailment [24-25].

Using multi-slice spiral CT scan, patients can obtain CT images of the whole lung by holding their breath at one time. The advancement of CT technology has resulted in an increase in its resolution, rendering CT scanning the preferred option for supplementary evaluation of LP in pediatric patients [26]. It can not only effectively solve the low detection rate of chest X-ray, but also judge whether there is other inflammation by three-dimensional reconstruction of the airway tree [26]. In addition, for doctors, the huge CT imaging data generated by the promotion of CT screening for LP in children brings a huge diagnostic workload [18, 27]. At present, most hospitals use radiologists to read films independently or use computer-aided detection and diagnosis system (CAD) to read films, and the screening work is mainly done manually by radiologists [28]. As early as the 1960s, foreign scholars invented the CAD system, adopted computer-aided radiological diagnosis, and applied it to the diagnosis of lung diseases [27]. The images on X-ray films were transformed into digital information that can be recognized and processed by the computer system, which made computer-aided radiological diagnosis possible and opened a new chapter of computer-aided medical diagnosis. Many scholars are interested in this direction. It paves the way for early screening of lung cancer in the future [29]. To date, numerous computer-aided diagnostic techniques have been devised that proficiently recognize the image data of chest X-ray, CT, and positron emission tomography (PET). These techniques can be employed to detect and categorize lung ailments in diverse image formats, thereby furnishing valuable assistance to radiologists in film interpretation and diagnosis [30-31].

According to the pathological characteristics of

the disease, the course of lobar pneumonia can be divided into three stages: exudation, consolidation and dissipation [32-33]. Among them, the consolidation stage can be divided into red and gray liver transformation stages.

The lesion of LP in the congestive phase indicated ground glass density shadow, and the edge of the lesion area was blurred [34]. During the consolidation phase, CT indicated that the dense consolidation shadow was distributed along the lobe and segment of the lung, in which the "air bronchus sign" was often seen [35]. Most of the patients with consolidation started from the periphery of the lung lobe and close to the pleura, and then gradually dispersed to the center of the lung field. After treatment, the lesion area of the patient was absorbed in varying degrees, and the CT plain scan indicated that the solid shadow density decreased until it was completely absorbed. The sensitivity, specificity and accuracy of chest CT plain scan were higher, and the positive predictive value was lower compared to the chest X-ray plain film diagnosis.

The positive predictive value of chest CT plain scan diagnosis was higher than that of chest X-ray plain film diagnosis. Based on AI and DL, the AUC of chest CT plain scan was 0.755 (95%CI was 0.657-0.852), and the AUC of chest X-ray was 0.625 (95%CI 0.486-0.764). It has been substantiated that chest radiography exhibits superior sensitivity and specificity in detecting LP in pediatric patients. Following treatment, the lesion is gradually reabsorbed, and both X-ray and CT scans are capable of effectively demonstrating this process. X-ray imaging is the preferred modality, while more severe cases may necessitate clinical reassessment based on individual patient circumstances.

CT examination time is short, multi-directional imaging and high image quality, obvious advantages in intuitive, multi-window display of different lung segments of the imaging findings, CT plain scan images of LP in children is not typical, observation of single lung texture increase, edge blur, consolidation and other image features cannot be qualitatively diagnosed, easy to be misdiagnosed as lobar atelectasis. Lobar atelectasis is a lobar disease, but the volume of LP is smaller than that of LP, and the adjacent organs are shifted to the lesion area. CT scan of LP in consolidation stage shows that dense consolidation is mostly distributed along the lobes and lung segments, and "air bronchus sign" is often seen in it. Most patients actually start from the periphery of the lung lobe and close to the pleura, and then gradually spread out to the center of the lung field. According to this characteristic, the two can be distinguished and diagnosed.

CONCLUSION

Taken together, Chest CT has high sensitivity and specificity in the diagnosis of LP in children, which can clearly demonstrate the imaging features of LP before and after treatment and provide reliable imaging data for clinic.

REFERENCES

1. Zinserling VA, Swistunov VV, Botvinkin AD, *et al.* (2022) Lobar (croupous) pneumonia: old and new data. *Infection,* **50**(1): 235-242.
2. Deng LN, Zhang GJ, Lin XQ (2021) Comparative study of energy spectrum and perfusion CT imaging in differential diagnosis of peripheral lung cancer and focal organized pneumonia [J/OL]. *Chinese Journal of Medical Imaging,* **12**: (09) 1-6.
3. Haghbayan M, Khatami S S, Nasrollahi Heravi F (2021) The estimation of newly infected cases of covid-19 with consideration of governmental action and behavior of people in Iran. *SJMSHM,* **3** (1): 1-7.
4. Yu YX, Li M, Gu L (2021) Study on early recognition of severe COVID-19 by nomogram based on clinical and CT features. *Journal of Clinical Radiology,* **40**: (06) 1106-1111.
5. Rujittika M and Viroj W (2021) Letter to the Editor: Quantitative evaluation of COVID-19 pneumonia severity by CT pneumonia analysis algorithm using DL technology and blood test results. *Japanese Journal of Radiology,* **39**: (10) 176-179.
6. Chen WT, Sun L, Tan AB (2021) Prediction of radiation pneumonitis in radiotherapy for lung cancer based on CT imaging characteristics and clinical physical dose characteristics. *Chinese Journal of Medical Physics,* **38**: (06) 672-676.
7. Wei J, Zhu RH, Zhang H (2021) Application of PET/CT image under convolutional neural network model in postoperative pneumonia virus infection monitoring of patients with non-small cell lung cancer. *Results in Physics,* **26**: (56) 34-38.

8. Shuang W, Yi Z, Liu YK (2021) Analysis of image features and TCM syndrome types of lobar pneumonia in children based on mean square deviation lung CT image registration algorithm. *Scientific Programming, 8: 2021*.

9. Mihaela RL (2021) DL in classification of covid-19 coronavirus, pneumonia and healthy lungs on CXR and CT images. *Journal of Medical and Biological Engineering, 5: (67) 166-169*.

10. Zhang MD, Yu SW, Yin XT (2021) An AI-based auxiliary empirical antibiotic therapy model for children with bacterial pneumonia using low-dose chest CT images. Japanese journal of radiology, 39: (10) 14-17.

11. Argentieri GL, Bellesi L, Pagnamenta A (2021) Diagnostic yield, safety, and advantages of ultra-low dose chest CT compared to chest radiography in early stage suspected SARS-CoV-2 pneumonia: A retrospective observational study. *Medicine, 100: (21) 566-569*.

12. Wang N, Hou ZB, Wang CX (2021) Diagnostic value of CTA in children with severe mycoplasma pneumonia complicated with vascular embolism. *Radiology Practice, 36: (05) 648-652*.

13. Konietzke P, Steentoft HaukH, Wagner WL (2021) Consolidated lung on contrast-enhanced chest CT: the use of spectral-detector computed tomography parameters in differentiating atelectasis and pneumonia. *Heliyon, 7: (5) 45-49*.

14. Jeroen CJ, Richard AT, Frans K, *et al.* (2020) Signs of pulmonary infection on admission chest computed tomography are associated with pneumonia or death in patients with acute stroke. *Stroke, 51:1690–1695*.

15. Romanov A, Bach M, Yang S (2021) Automated CT lung density analysis of viral pneumonia and healthy lungs using DL-based segmentation, histograms and HU thresholds. *Diagnostics (Basel, Switzerland), 11: (5) 54-58*.

16. Ma MT, Xie Q, Wang WL (2021) Comparison of the value of chest plain film, pulmonary ultrasound and CT in the diagnosis of pneumonia in children . *Chinese CT and MRI Magazine, 19: (05) 30-32*.

17. Yazaki K, Nonaka M, Shigemasa R (2021) Usual interstitial pneumonia progressing to nonspecific interstitial pneumonia-like pattern on high-resolution CT with histologic confirmation. *Radiology Case Reports, 16: (5) 14-19*.

18. Lu S, Xing ZH, Zhao SY (2021) Different Appearance of Chest CT Images of T2DM and NDM Patients with COVID-19 Pneumonia Based on an Artificial Intelligent Quantitative Method. *International Journal of Endocrinology, 21: (62) 34-39*.

19. Das KM, Alkoteesh JA, Al KJ (2021) Comparison of chest radiography and chest CT for evaluation of pediatric COVID-19 pneumonia: Does CT add diagnostic value? *Pediatric Pulmonology, 56: (6) 43-46*.

20. Auspicious L, Lei ZX, Wu SY (2021) Clinical and hematological characteristics of bronchopneumonia and LP in children with mycoplasma pneumoniae infection. *Chinese Journal of Hospital Epidemiology, 31: (02) 281-285*.

21. Wang J, Xia C, Sharma A (2021) Chest CT Findings and Differential Diagnosis of Mycoplasma pneumoniae Pneumonia and Mycoplasma pneumoniae Combined with Streptococcal Pneumonia in Children. *Journal of Healthcare Engineering, 201: (5) 18-21*.

22. Savelli G, Bonacina M, Rizzo A (2020) Activated macrophages are the main inflammatory cell in COVID-19 interstitial pneumonia infiltrates. Is it possible to show their metabolic activity and thus the grade of inflammatory burden with 18 F-Fluorocholine PET/CT? *Medical Hypotheses, 144: (6) 856-859*.

23. Capristo C and Rossi GA (2017) Post-infectious persistent cough: pathogenesis and therapeutic options. *Minerva Pediatr, 69: (5) 444-452*.

24. Martini K, Blüthgen C, Walter JE (2020) Accuracy of Conventional and Machine Learning Enhanced Chest Radiography for the Assessment of COVID-19 Pneumonia: Intra-Individual Comparison with CT. *Journal of Clinical Medicine, 9: (11) 784-789*.

25. Li WQ, Chen Y, Fu AS (2020) Serum procalcitonin, smoking history combined age established a new prediction model for predicting dynamic changes of chest CT images in adult community-acquired pneumonia (CAP) Patients. Clinical laboratory, 66: (11) 86-89.

26. Lung D and Conditions VP (2020) New viral pneumonia study results reported from respiratory intensive care unit (Atomatic Detection and Diagnosis of Severe Viral Pneumonia Ct Images Based On Lda-svm). *Journal of Robotics & Machine Learning, 64: (4) 112-115*.

27. Coronavirus - COVID-19 (2021) Findings from Shahid Beheshti University of Medical Sciences Provides New Data on COVID-19 (Risk Factors for Poor Outcome in Patients with Severe Viral Pneumonia on Chest CT during the COVID-19 Outbreak: a Perspective from Iran). *Medical Letter on the CDC & FDA, 46: (3) 156-158*.

28. Wang Y, Wu B, Zhang N, *et al.* (2020) Research progress of computer aided diagnosis system for pulmonary nodules in CT images. *J Xray Sci Technol, 28: (1) 1-16*.

29. AI (2020) New AI Study Findings Have Been Reported from Shenzhen University (Using AI To Detect Covid-19 and Community-acquired Pneumonia Based On Pulmonary Ct: Evaluation of the Diagnostic Accuracy). *Medical Letter on the CDC & FDA, 30: (13) 145-148*.

30. Tianyu X, Zhang WT, Qian BY (2020) The role and challenge of AI in new coronavirus pneumonia CT diagnosis. *TMR Modern Herbal Medicine, 30: (3) 156-158*.

31. Moritz S, Katharina M, Stephan S (2020) Pneumonia detection in chest X-ray dose-equivalent CT: impact of dose reduction on detectability by AI. *Academic Radiology, 28: (67) 144-148*.

32. Yue HM, Qian Y, Liu C (2020) Machine learning-based CT radiomics method for predicting hospital stay in patients with pneumonia associated with SARS-CoV-2 infection: a multicenter study. *Annals of Translational Medicine, 8: (14) 45-48*.

33. Gao Y and Ren HF (2019) Analysis of the value of 64-slice CT thin-layer reconstruction and HRCT in the diagnosis of MP pneumonia in children. *Chinese CT and MRI Magazine, 17: (12) 56-58+163*.

34. Xu HF, Yang Y, Zhang XR (2017) CT findings of mycoplasma pneumoniae lung abscess in children (analysis of 12 cases). *Radiology Practice, 32: (10) 1057-1059*.

35. Zhang Y, Shang W, Song XM (2017) Differential diagnosis of Mycoplasma pneumoniae pneumonia and Mycoplasma pneumoniae complicated with Streptococcus pneumoniae pneumonia by chest CT in Children. *Chinese Journal of Hospital Epidemiology, 27: (06) 1391-1393+1397*.